UDC 621.575:620.91:662.997
DOI: 10.15587/1729-4061.2021.229545

IMPROVING ENERGY EFFICIENCY OF THE SYSTEMS FOR OBTAINING WATER FROM ATMOSPHERIC AIR

Nataliia Bilenko
Postgraduate Student*
E-mail: natalibilenco@gmail.com
Oleksandr Titlov
Doctor of Technical Sciences, Professor,
Head of Department*
E-mail: titlov1959@gmail.com
*Department of Oil and Gas Technologies,
Engineering and Power Engineering
Odessa National Academy
of Food Technologies
Kanatna str., 112, Odessa, Ukraine, 65039

This paper outlines the prospect of obtaining water from atmospheric air by cooling it to the dew point temperature using refrigeration machines in order to partially reduce water scarcity in the arid regions of our planet. To minimize energy costs in the systems for obtaining water from atmospheric air, it is proposed to utilize solar energy with absorption refrigeration units (ARUs) acting as a source of artificial cold.

The characteristic thermodynamic processes have been analyzed in a modernized ARU, capable of working at a lower thermal energy source's temperature than its analogs. The possibility has been studied to reduce the temperature of the heat source by including a solution vaporizer in the ARU scheme. The analysis involved an authentic method based on the balance of specific streams of ARU working body components and actual boundary conditions at characteristic points of the cycle. A limit was shown for the level of a minimum boiling temperature in the ARU generator (from 90 °C) when the systems for obtaining water from atmospheric air are operated under current climatic conditions.

The simulation of heat-and-mass exchange processes during contact interaction between a steam-gas mixture and ammonia water solution was carried out.

Based on variant calculations, it has been shown that the proposed ARU structure with an adiabatic solution vaporizer could work as part of systems to obtain water from atmospheric air at a hot spring temperature above 100 °C and constructively enough fits into the element base of standard models.

It has been proposed to use two types of solar thermal energy sources to operate ARU. In a tropical climate, with vacuum solar collectors or solar energy hubs; in a temperate climate zone, with solar collectors with water as a heat carrier

Keywords: water from atmospheric air, refrigeration machines, absorption refrigeration units, solar energy

Received date 19.11.2020
Accepted date 21.01.2021
Published date 30.04.2021

How to Cite: *Bilenko, N., Titlov, O. (2021). Improving energy efficiency of the systems for obtaining water from atmospheric air. Eastern-European Journal of Enterprise Technologies, 2 (8 (110)), 31–40. doi: https://doi.org/10.15587/1729-4061.2021.229545*

1. Introduction

It is becoming clear to the world community that very soon water will be the most valuable resource on the planet. In the future, the struggle for water resources in the world will become a factor in armed conflicts; this trend will only accelerate in the near future.

To help address this problem, the United Nations General Assembly declared 2005–2015 the International Decade of Water for Life [1].

About 70 percent of the world's surface is covered with water, but 97.5 percent is saltwater.

Known methods of seawater desalination (thermal-evaporation or crystallization; membrane; ion exchange; electrodialysis; reverse osmosis; combined [2]) partially solve water supply problems but are characterized by high energy and resource costs.

Meanwhile, the main part of freshwater is in a 1-kilometer layer of the atmosphere. According to work [3], the average absolute humidity near the earth's surface is 11 g/m^3, and in tropical regions, it reaches 25 g/m^3 and above.

Many countries in the tropical zone suffer from a lack of freshwater, although its atmospheric content is very high.

Therefore, one of the most important tasks for the world community is the development of technologies that would make it possible to extract water from the air, and directly at the place where it is necessary.

2. Literature review and problem statement

Since ancient times, freshwater has been obtained by collecting condensed droplets from the air as a result of the natural daily radiation cooling of the earth's surface in very limited quantities [4].

It is known [5] that if the temperature drops by 10 to 15 °C, 10 to 14 grams of water could be received from each cubic meter.

Intensifying elements are used to increase the condensation of water vapor in natural conditions. First of all, these include cold-accumulators (rubble) [6] and heat pipes that provide heat transmission over considerable distances. Solid sorbents, which work under a cyclical mode of "charge-discharge" are also used [7].

The disadvantages of known techniques [4–7] to obtain water in natural conditions include the dependence on the thermal parameters of atmospheric air that vary during the day and time of year.

The main share of the market for systems for obtaining water from atmospheric air belongs to models that include a vapor compression refrigeration machine (VCRM) [8]. VCRMs are equipped with an electric drive and are guaranteed to provide a temperature below the dew point in a wide range of the heat-moisture parameters of atmospheric air.

At the same time, the use of specialized systems with VCRM [8] is promising only for the performance of up to

3–4 liters of water per hour. With higher performance, there is a significant increase in the size of the installation to obtain water from atmospheric air.

At the same time, compression refrigeration machines [9] and thermoelectric coolers [10] are successfully applied in home solar-powered air conditioning systems. This refrigeration equipment could be adapted with a small modernization for the task of obtaining water from atmospheric air.

However, the disadvantage of such photo-voltaic systems [9, 10] is their cost, which exceeds that of the systems powered by AC current from the grid.

A significantly higher, in comparison with compression analogs, productivity of systems for obtaining water from atmospheric air can be achieved with adiabatic expansion in a turboexpander of an air refrigeration machine. Such machines are successfully used in space technology to launch aircraft [11].

However, there are many places in the world, including the countries of North Africa, Southeast Asia, Central and South America, which face, in addition to water scarcity, problems with electricity. In addition, given the depletion of the planet's oil and gas resources, the utilization of electricity on water generation systems becomes impractical. Similar problems are common in the southern region of Ukraine [12].

In this regard, designers and researchers of systems for obtaining water from atmospheric air pay considerable attention to heat-using cold generators whose source of heat is solar energy. One promising direction is the possibility of using available solar collector infrastructure.

Among heat-using cold generators, designers look at sorption schemes – with a solid absorber (adsorption type) and a liquid absorber (absorption type).

The disadvantages of modern adsorption schemes include their link to the liquid cooling systems of heat-scattering elements (a capacitor and an adsorber), which involve cooling towers and water loss during evaporative cooling. Undoubtedly, this makes it impossible to use them in arid regions where there is a water shortage.

One can note among the absorption refrigeration systems used in technologies for obtaining water from atmospheric air those schemes that involve an ammonia-water solution (AWS) as a working body [14–16]. These systems are successfully operated by air-draining heat from heat-scattering elements, in particular, pump-free schemes with inert gas.

However, additional special solar energy concentration systems are needed for their work [14, 15], or vacuum solar collectors with a high-boiling heat-carrier [16].

Widespread use of absorbent ammonia-water refrigeration systems in the schemes for obtaining water from atmospheric air is limited due to insufficient temperature levels of the solar energy source. This is because currently the main fleet of solar collectors is made up of structures where water is a heat carrier. The practical heating temperature in such systems does not exceed 100 °C. This is not enough to implement the absorption cycle even in the temperate climate zone both for the pumping scheme (an optimal working range of 120–140 °C) and the pump-free scheme (an optimal working range of 150–170 °C).

To solve the task of lowering the temperature level of the heat source to the required level, the pumping schemes of absorbent refrigeration machines include a special pressing booster compressor [18]. This reduces the heat source level to 70 °C [19] but requires electrical energy to drive the booster compressor, which reduces autonomy during operation.

The operational autonomy of the cold source in the systems for obtaining water from atmospheric air can be ensured by an original pump-free absorption refrigeration unit (ARU) [20]. ARU, according to the author, could use a heat source with a temperature of 75 °C, which would make it possible to utilize a budget solar collector with water as a heat carrier.

The problem with the use of ARU [20] is the uncertainty of operating modes – unknown temperatures of the ambient air and cooled object.

Thus, in order to address the issue related to the widespread use of low-potential heat sources, such as solar water collectors with water as a heat carrier, in the systems for obtaining water from atmospheric air, appropriate research into the working patterns of ARU's prospective schemes is necessary. One such promising scheme is the ARU [20] based on solar collectors with water as a heat carrier.

It should also be noted that the working body of absorption refrigeration systems of the pump and pump-free types is a natural working body – AWS, which does not have an adverse technogenic impact on the planet's ecosystem [21]. In addition, ammonia makes it possible to expand the scope of their use in terms of reducing the temperature of a cold source below 0 °C, for example, to solve the tasks of air conditioning or low-temperature storage of food and raw materials.

3. The aim and objectives of the study

The purpose of this study is to increase the energy efficiency of systems for obtaining water from atmospheric air by improving the thermodynamic cycle and ARU elements that operate from low-potential thermal energy sources.

To accomplish the aim, the following tasks have been set:

– to conduct thermodynamic analysis of the ARU cycle and to determine ways to reduce the temperature of the source of heat load in the climatic conditions of the systems for obtaining water from atmospheric air;

– to perform a structural calculation of the elements of ARU that operates from low-potential thermal energy sources.

4. Materials and methods to study the thermodynamic parameters of an autonomous absorption refrigeration unit cycle

The object of our study is an absorption refrigeration unit (ARU) that operates at lower, compared to analogs, heat source temperatures [20].

The main ARU elements are generator node 1, dephlegmator 2, capacitor 3, ammonia vaporizer 4, absorber 5, and ammonia water solution vaporizer 6 (Fig. 1).

The generator node includes boiler-steam-generator 7 (hereafter, generator), liquid separator 8, the channels of weak and strong AWS 9 and 10. All elements of the generator node and, partially, dephlegmator 2 at the bottom are covered with insulation casing.

A conventional working body for ARU is AWS with the addition of inert gas (hydrogen, helium, or their mixture). Ammonia is a refrigeration agent; water is an absorbent. When refueling, the mass share (by ammonia) of AWS, depending on the functional purpose of conventional ARUs, varies from 30 to 36 % [22].

Typically, the work of heat-scattering elements of ARU (capacitor 3, absorber 5, and dephlegmator 2) takes place under the mode of natural-convective and radiation cooling. That improves reliability and increases operational resource but forces designers to provide for a high enough level of pressure in ARU in order to ensure acceptable mass-dimension indicators.

Increased pressure in the system makes it possible to increase the temperature of the phase transition (condensation) of ammonia, as well as a temperature difference with the environment, and, accordingly, reduce the size of the heat discharge zone.

In ARU models that are designed to operate in temperate climates, the absolute pressure is about 20 bar, in a tropical climate ≈30 bar [22].

To improve the energy efficiency of ARU, the scheme includes three regenerative heat exchangers: 11 – liquid solutions; 12 and 13 – steam-gas mixture.

The amount of refueling is selected in such a way that under a working mode the level ▼1 provides the AWS feed through AWS vaporizer 6, and the heat exchanger of solutions 11 – to the inlet of absorber 5 (▼1>▼2).

The generator in this scheme performs two functions – a boiler-steam-generator and a device for lifting liquid (a pump-thermosyphon) from level ▼3 (absorber output) to level ▼1. The inner diameter of a generator tube in modern ARUs is 2.0...2.5 mm [23].

When refueling, ARU is vacuumed, then it is filled with the estimated amount of liquid AWS, and, at the last stage, with an inert gas such as hydrogen. In non-working conditions, hydrogen fills dephlegmator 2, capacitor 3, vaporizers 4 and 6, absorber 5, and heat exchangers 12 and 13.

When the heat is supplied, vapor bubbles form in the lower part of generator 7, consisting mainly of ammonia. Under the influence of lifting force, vapor bubbles carry the ammonia-depleted liquid into the upper part of the generator.

From the top of generator 1, the vapor-liquid mixture enters separator 8 where the liquid phase (a weak solution) flows into channel 8, and then into the heat exchanger of solutions 11; steam enters dephlegmator 2.

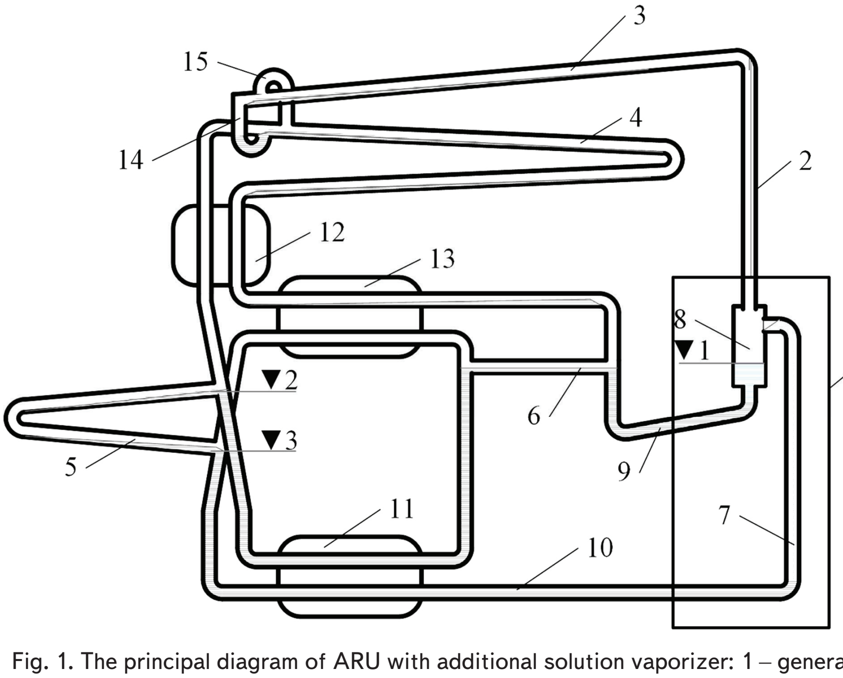

Fig. 1. The principal diagram of ARU with additional solution vaporizer: 1 – generator node; 2 – dephlegmator; 3 – capacitor; 4 – ammonia vaporizer; 5 – absorber; 6 – solution vaporizer; 7 – generator; 8 – separator; 9 – the channel of weak AWS; 10 – the channel of strong AWS; 11 – heat exchanger for solutions; 12, 13 – SGM heat exchangers; 14 – ammonia hydraulic seal; 15 – leveling pipe; ▼1, ▼2, ▼3 – the levels of a weak solution in the separator, at the inlet and outlet of the absorber, respectively

After some time after starting work, the weak AWS completely fills channel 9 to level ▼2 and begins to flow to the top of absorber 5. With constant use of ARU, the channel of the weak AWS in ARU is always filled with solution up to level ▼2.

In the heat exchanger of solutions 11, the flow of weak AWS gives heat to the flow of strong AWS, going to meet it from the receiver to the rectifier. Next, the flow of weak AWS is further cooled before entering the absorber in the process of heat exchange with external air.

In separator 8, the vapor created pushes out hydrogen from dephlegmator 2 and capacitor 3 into ammonia vaporizer 4 and absorber 5.

Liquid ammonia is fed to the initial section of ammonia vaporizer 4 through hydraulic seal 14 from capacitor 3, and, from absorber 5 – purified vapor gas mixture. To level the pressure on both sides of hydraulic seal 14 and stabilize the supply of liquid ammonia to vaporizer 4, leveling pipe 15 is used. Liquid ammonia comes into contact with the steam-gas mixture (SGM), consisting mainly of hydrogen. Upon contact, it evaporates intensely into the inert gas environment at low partial pressures and, accordingly, at low temperatures.

The partial pressure of ammonia and the temperature of evaporation increase as ammonia flows, that is the generation of artificial cold in the ARU vaporizer is carried out at a variable temperature – from the minimum to the maximum.

With a greater density compared to hydrogen, ammonia-rich SGM from vaporizer 4 through heat exchangers 13 and 14 and solution vaporizer 6 descends into the lower part of absorber 5. When moving, the saturated SGM pushes out of absorber 5 into the ammonia vaporizer 4 purified SGM, containing mainly hydrogen.

Thus, due to the difference in SGMs densities, a contour of the natural circulation between the vaporizer and the absorber is formed.

In the vaporizer of solution 6, the flow of cold SGM under a direct current mode comes into contact with the weak AWS. As a result of the heat-and-mass exchange, SGM is further saturated with ammonia and heated, and the weak AWS, on the contrary, cools and becomes less saturated by ammonia.

Such a scheme of ARU with a vaporizer of solutions, according to the author of [20], makes it possible to reduce the temperature of the heat source to 75 °C by operating with a more ammonia-saturated AWS.

The flow of SGM, heated in solution vaporizer 6, is partially cooled in heat exchanger 13 and passes on to the lower part of absorber 5.

In absorber 5, SGM comes into contact with the weak ammonia AWS, which comes from generator 1 through solution vaporizer 6 and solution heat exchanger 11. The absorption of ammonia vapor from SGM occurs in the absorber by the weak AWS under a counter-current mode with SGM. The heat of the mixing (absorption) is diverted to the environment.

The ammonia-treated SGM flow returns to ammonia vaporizer 4, and, before contact with liquid ammonia, there is some cooling during the heat exchange with cold SGM in heat exchanger 12.

Ammonia-rich strong AWS through the heat exchanger of solutions 11 enters the inlet of the generator. Then the ARU cycle repeats itself.

As noted above, the author of the design described in [20] reported on the possibility of ARU working with a temperature source of 75 °C. However, at the same time, there is no information – in what climatic conditions of operation and with what level of cooling temperatures this possibility was achieved.

For the task of obtaining water from the atmospheric air by condensation at the temperature of the “dew point”, there are certain introductory positions on these parameters. These include, first of all, recommendations on heat-moisture modes in regions with the predominant use of systems for obtaining water from atmospheric air [24]: an ambient temperature of 32–34 °C and a dew point temperature of up to 15 °C. For such operating conditions of the scheme given in [20], taking into account our experience [25, 26], as well as the results from experimental work by other researchers [27–38], we can accept the initial data parameters:

a) a lower (higher) evaporation temperature $\nu_{\min}(\nu_{\max})$ of minus 5 °C (5 °C);

b) full pressure in ARU, which ensures the condensation of ammonia vapor when heat is diverted to the environment under a natural convection mode is P=2.0 MPa;

c) the difference in the pressures of the saturated ammonia liquid and the partial pressure of ammonia vapor in SGM at the inlet of the vaporizer – the outlet of the absorber is ΔP_H=0.10 MPa, and at the outlet of the vaporizer – the inlet to the solution vaporizer is ΔP_B=0.05 MPa; ΔP_B=0.35 MPa;

d) the difference of the partial pressure of ammonia vapor in SGM and the pressure of the saturation of a weak (strong) AWS in the absorber is 0.10 (0.05) MPa;

e) the temperature of the environment (atmospheric air) is t_a=32 °C);

f) the temperature difference between the environment and the absorber’s wall at the inlet and outlet of the AWS is, respectively, Δt_1=10 °C and Δt_2=14 °C.

The characteristic points of the ARU cycle with an additional solution vaporizer are shown in Fig. 2.

The task of the calculation is to find an answer to the question of whether ARU with an additional vaporizer of solutions could provide for the generation of artificial cold for the systems for obtaining water from atmospheric air under the given initial parameters.

A variable parameter in the calculation is the maximum and minimum temperature of the heat source.

In the first step, we find the following:

a) liquid ammonia saturation pressure:

1) the lowest at the beginning of the evaporation process

$$P_H = f_1(v_{\min}); \qquad (1)$$

2) the highest at the end of the evaporation process

$$P_B = f_1(v_{\max}); \qquad (2)$$

b) the partial pressure of ammonia vapor in an SGM flow at the beginning and end of evaporation

$$P_{x(\min)} = P_H - \Delta P_H, \qquad (3)$$

$$P_{x(\max)} = P_B - \Delta P_B; \qquad (4)$$

c) the partial pressure of inert gas in an SGM flow at the beginning and end of evaporation

$$P_{G(\min)} = P - P_{x(\min)}, \qquad (5)$$

$$P_{G(\max)} = P - P_{x(\max)}; \qquad (6)$$

d) the volumetric share of ammonia in an SGM flow at the beginning and end of evaporation

$$\varphi_{x(\min)} = \frac{P_{x(\min)}}{P}, \qquad (7)$$

$$\varphi_{x(\max)} = \frac{P_{x(\max)}}{P}; \qquad (8)$$

e) the mass share of ammonia in an SGM flow at the beginning and end of evaporation

$$\xi_{x(\min)} = \left[\left(\frac{1}{\varphi_{x(\min)}} - 1\right)\frac{\mu_G}{\mu_x} + 1\right]^{-1}, \qquad (9)$$

$$\xi_{x(\max)} = \left[\left(\frac{1}{\varphi_{x(\max)}} - 1\right)\frac{\mu_G}{\mu_x} + 1\right]^{-1}, \qquad (10)$$

where μ_G=2 and μ_x=17 are the molecular masses of inert gas (hydrogen) and the refrigeration agent (ammonia), respectively.

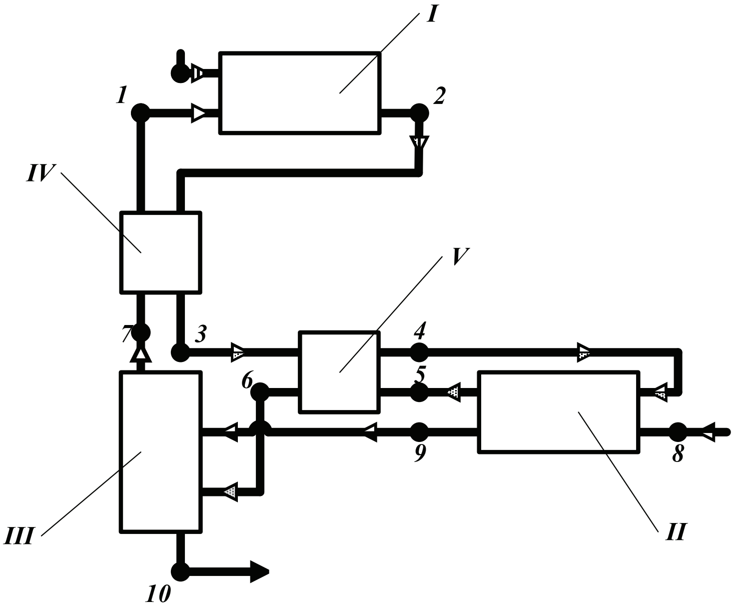

Fig. 2. Characteristic points of the ARU cycle with an additional solution vaporizer: 1–10; I – ammonia vaporizer; II – solution vaporizer; III – absorber; IV, V – SGM heat exchangers; ▶ – a stream of strong AWS; ◁ – a flow of maximally-saturated SGM; ▷ – a stream of liquid ammonia; ▷ – a stream of saturated SGM; ◀ – a stream of purified AWS; ◀ – a stream of weak AWS

5. Results of the thermodynamic analysis of the ARU cycle

Our calculation, according to the above algorithm, is carried out for 1 kg of evaporating ammonia, which makes it possible, taking into consideration the values of $\xi_{x(\min)}$ and $\xi_{x(\max)}$, to determine the following:

a) a specific amount of circulating (ballast) ammonia in an SGM flow between the vaporizer and absorber

$$M_X = \frac{B}{A-B}, \tag{11}$$

where

$$A = \frac{1-\xi_{x(\min)}}{\xi_{x(\min)}}, \quad B = \frac{1-\xi_{x(\max)}}{\xi_{x(\max)}};$$

b) a specific amount of circulating inert gas in an SGM flow between the ammonia vaporizer and absorber according to the conventional scheme of operation (without a solution vaporizer)

$$M_G = M_X A. \tag{12}$$

In the second stage, we determine the temperature at the characteristic points (at the inlet and outlet of the absorber):

a) the flow of weak AWS at the inlet to the absorber

$$T'_A = t_a + \Delta t_1; \tag{13}$$

b) the flow of strong AWS at the outlet of the absorber

$$T''_A = t_a + \Delta t_2. \tag{14}$$

The temperature and formulation of the weak AWS determine the degree of SGM purification in the absorber and the minimum temperature in the ammonia vaporizer.

In a given case: $T'_A = 32+10 = 42\,^{\circ}\text{C}$; $T''_A = 32+14 = 46\,^{\circ}\text{C}$.

Using reference data from [39] and the initial parameters, we find: P_H=0.35 MPa; P_B=0.52 MPa; $P_{x(\min)}$=0.30 MPa; $P_{x(\max)}$=0.47 MPa.

Thus, at the inlet of the absorber, the flow of weak AWS with a temperature of 42 °C and saturation pressure of 0.20 MPa should have a mass share for ammonia $\zeta'_W = 0.31$ (point 9 in Fig. 2).

At the maximum boiling point of AWS in the generator of $t_{\max=}$80; 90; 100 °C (point 8 in Fig. 3), the mass share of weak AWS for ammonia [39] is, respectively, ξ_W=0.58; 0.51; 0.44. The minimum boiling point was accepted to equal 70 °C (strong AWS with a mass share of ammonia ξ_f =0.67 at a pressure in the system P=2.0 MPa).

Such formulation of weak AWS does not meet the requirement for SGM purification in the absorber (0.31 for ammonia), which predetermines the introduction of an additional solution vaporizer in the ARU scheme (position II in Fig. 3).

When calculating the vaporizer of solutions, it is necessary to ensure its modes of operation in such a way as to prevent additional absorption of ammonia vapor by weak AWS. To this end, the pressure of saturation of weak AWS should be higher than the partial pressure of vapor of ammonia in SGM.

To determine the specific amount of ammonia that needs to be extracted from the weak AWS to meet the requirements for the formulation of the mixture at the inlet to the absorber $(\zeta'_W = 0.31)$, we find the AWS circulation multiplicity

$$f = \frac{1-\xi_W}{\xi_f - \xi_W}. \tag{15}$$

We find a specific amount, respectively, of ammonia and water in weak AWS coming out of the generator (point 8 in Fig. 2)

$$M'_A = f \cdot \xi_W, \tag{16}$$

$$M'_B = f - M'_A. \tag{17}$$

Knowing the quantitative composition of AWS at the inlet to the vaporizer of solutions and the condition $\zeta'_W = 0.31$, one could find the specific amount of ammonia $\left(M''_A\right)$ in the AWS after purification (point 9, Fig. 2) from the following ratio

$$\xi'_W = \frac{M''_A}{M''_A + M'_B}. \tag{18}$$

Then the specific amount of ammonia, which passed into SGM in the vaporizer of solutions is

$$\Delta M_A = M'_A - M''_A. \tag{19}$$

Taking into consideration ratios (11), (12), and (22), we find a new formulation of SGM at the output of the vaporizer of solutions

$$\bar{M}_A = M_x + \Delta M_A, \tag{20}$$

$$\bar{M}_M = \bar{M}_A + M_G. \tag{21}$$

The mass share of ammonia vapor in SGM at the output of the solution vaporizer

$$\bar{\xi}_A = \frac{\bar{M}_A}{\bar{M}_M}. \tag{22}$$

The volumetric share of ammonia in SGM at the outlet of the solution vaporizer is found from the following equation

$$\bar{\varphi}_A = \frac{1}{\left(\frac{1-\bar{\xi}_A}{\bar{\xi}_A}\right)\cdot\frac{\mu_x}{\mu_G}+1}. \tag{23}$$

The partial pressure of ammonia vapor in SGM at the outlet of the solution vaporizer is

$$\bar{P}_A = P_o \cdot \bar{\xi}_A. \tag{24}$$

To prevent the absorption process in the section of the solution vaporizer, it is necessary that the partial pressure of the ammonia vapor in SGM is greater than the pressure of the saturation of additionally purified weak AWS at $\xi'_W = 0.31$, that is

$$P^s_{W-A} \succ \bar{P}_A. \tag{25}$$

In turn, the pressure of AWS saturation depends on the composition of the mixture and temperature; in this case, on the numerical value of the temperature. Using the estimation ratios from [40], we obtained the numerical values of the equilibrium temperature that met condition (25).

For $t_{\max}$=80; 90; 100 °C, the equilibrium temperature was, respectively, 87; 85; 80 °C.

The necessary level of equilibrium temperatures could be provided only at the expense of a warming heat source. It is obvious that at the maximum boiling point in the generator of 80 °C, the level of equilibrium temperature in the solution vaporizer of 87 °C cannot be provided.

The necessary condition (25), in this case, can be met only at the level of maximum boiling temperatures in the generator not lower than 90 °C. At a total pressure of 2.0 MPa in the system, this corresponds to the mass fraction of weak AWS ξ_W=0.51. With an increase in $t_{\max}$ to 100 °C, ξ_W would decrease to 0.44.

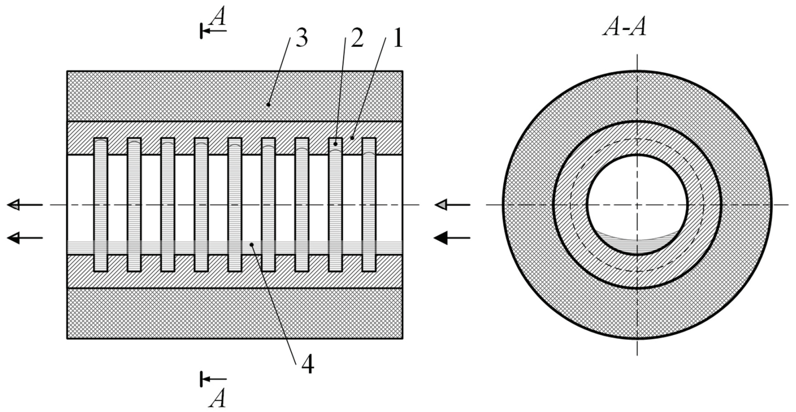

Fig. 3. The scheme of the solution vaporizer in the modernized ARU: *a* – a general view; *b* – A-A cross-section; 1 – hull; 2 – radial groove capillary structure; 3 – insulation casing; 4 – liquid AWS flow

6. Results of a structural calculation of the elements of ARU operated on low-potential thermal energy sources

Appropriate analytical studies have been conducted to assess the possible geometric parameters of the solution vaporizer in the upgraded ARU, which could meet the requirements for AWS purification.

The task set was to perform structural calculations of the cylindrical solution vaporizer with a direct-flow movement of the working body's phases – the inlet receives purified SGM and weak AWS, the outlet produces saturated SGM and purified AWS.

Underlying the test calculation of the ARU solution vaporizer is a mathematical model of the heat-and-mass exchange processes (the flow scheme is shown in Fig. 3).

To induce the gravitational flow of liquid AWS 4, the tube of solution vaporizer 1 is installed at some angle to the horizon (2...3° [41]).

In order to intensify the heat-mass exchange process between the streams of the working body, the inner surface of the tube has grooved capillary structure 2, widely used in the designs of ARU vaporizers and absorbers [25]. This structure makes it possible for the liquid to coat up to 80 % of the inner surface of the solution vaporizer tube [41].

When executing a cycle of the modernized ARU, the result of contact interaction of the flows of the working body is the evaporation of ammonia from AWS into purified SGM. The driving force behind the evaporation process is the difference in ammonia compositions of SGM and AWS.

The result of the evaporation of ammonia from AWS to SGM is the partial cooling of the flows of liquid and SGM. To minimize heat losses to the environment, the solution vaporizer is covered by insulation casing 3.

The system of equations, which describe the processes of heat and mass exchange along the elementary section of the solution vaporizer *dx*, takes the following form:

a) the mass balance equation:

$$G_0 \cdot dY = k_A \cdot \left(y^* - y''\right) \cdot \psi \cdot dF; \qquad (26)$$

b) the equation of heat balance between SGM and AWS flows:

$$G_0 \cdot C'_p \cdot dt = \alpha \cdot \left(\vartheta - t\right) \cdot \psi \cdot dF. \qquad (27)$$

The equation of thermal balance along the section *dx*:

$$G_o \cdot r \cdot dY = -\left(G_o \cdot c'_p \cdot dt + G_{WA} \cdot c_{WA} \cdot d\vartheta\right), \qquad (28)$$

where:

– k_A is the mass transfer factor when ammonia vapor evaporates from weak AWS in SGM;

– α is the factor of convective heat exchange between AWS and SGM flows;

– t is the current SGM flow temperature;

– ϑ is the current temperature of AWS flow;

– G_0 is the mass flow rate of inert hydrogen gas, kg/s;

– Ψ is the surface of heat exchange per unit of the surface of phase contact (a liquid and SGM);

– $dF=dx\cdot\pi\cdot d$ is the area of the elementary section of the inner surface of the solution vaporizer tube, m^2;

– G_{WA} is the current mass AWS flow rate, kg/s;

– C_{WG} is the mass heat capacity of SGM;

– y'' is the current mass share of ammonia in SGM;

– y' is the current mass share of ammonia in AWS;

– y^* is the current mass share of ammonia in SGM in equilibrium with the saturated AWS liquid at temperature υ and the mass share of liquid ammonia y';

– Y is the current mass share of ammonia in SGM, which is the ratio of ammonia mass to the mass of the gas carrier (hydrogen);

– C'_p is the specific mass heat capacity of SGM, J/(kg·K);

$$C'_p = C'_{p(A)} \cdot Y + C'_{p(W)}\left(1 - Y\right), \qquad (29)$$

where $C'_{p(A)}$, $C'_{p(W)}$ are the specific mass heat capacity of, respectively, ammonia and hydrogen, J/(kg·K).

System (26) to (28) also includes the equation of the relationship between the formulation of SGM in different forms:

$$Y = \frac{y''}{1 + y''} \qquad (30)$$

and the AWS phase equilibrium:

$$y^* = f\left(y', \vartheta\right). \qquad (31)$$

When the absence of evaporation from the absorber (of water) is assumed, system (26) to (31) includes a balance equation:

$$G_o \cdot dY = dG_{WA}. \tag{32}$$

The original data for the design calculation of the ARU solution vaporizer are:

a) the mass AWS flow rate at the inlet to the solution vaporizer G'_{WA};

b) the mass SGM flow rate at the input of the solution vaporizer G'_{WG};

c) absolute pressure in the system P_o;

d) the mass proportion of ammonia in AWS at the inlet of the solution vaporizer y';

e) the mass proportion of ammonia in SGM at the inlet of the solution vaporizer y'';

f) t_1 is the temperature of SGM flow at the inlet of the solution vaporizer;

g) ϑ_1 is the temperature of AWS flow at the inlet of the solution vaporizer.

When solving this problem, differential equations (26) to (28), included in system (26) to (31), were represented in the following form.

$$G_0 \cdot \frac{dY}{dF} = K_A \cdot \left(y^* - y''\right) \cdot \psi, \tag{33}$$

$$G_0 \cdot c'_p \cdot \frac{dt}{dF} = \alpha \cdot \left(\vartheta - t\right) \cdot \psi, \tag{34}$$

$$G_{WA} \cdot c_{p(WA)} \cdot \frac{d\vartheta}{dF} = -G_0 \cdot c'_p \cdot \frac{dt}{dF} - G_0 \cdot r \cdot \frac{dY}{dF}. \tag{35}$$

Given that for an elementary section of length dx

$$dF = \pi \cdot d \cdot dx \tag{36}$$

system (26) to (28) can be written as:

$$\frac{dY}{dx} = a \cdot \left(y^* - y''\right), \tag{37}$$

$$\frac{dt}{dF} = b \cdot \left(\vartheta - t\right), \tag{38}$$

$$\frac{d\vartheta}{dx} = -A \cdot \left(\vartheta - t\right) - B \cdot \left(y^* - y''\right), \tag{39}$$

where

$$a = \frac{K_A \cdot \psi \cdot \pi \cdot d}{G_0}, \tag{40}$$

$$b = \frac{\alpha \cdot \psi \cdot \pi \cdot d}{G_0 \cdot c'_p}, \tag{41}$$

$$A = \frac{\alpha \cdot \psi \cdot \left(\pi \cdot d\right)^2}{G_{WA} \cdot c_{p(WA)}}, \tag{42}$$

$$B = \frac{K_A \cdot \psi \cdot \left(\pi \cdot d\right)^2}{G_{WA} \cdot c_{p(WA)}}. \tag{43}$$

Using Euler's method and by assigning the increment Δx, we find an increment of functions (37) to (39)

$$\Delta Y = a \cdot \left(y^* - y''\right) \cdot \Delta x, \tag{44}$$

$$\Delta t = b \cdot \left(\vartheta - t\right) \cdot \Delta x, \tag{45}$$

$$\Delta\vartheta = -P \cdot \Delta t - R \cdot \Delta Y, \tag{46}$$

where

$$P = \frac{A}{b}; \;\; R = \frac{B}{a}. \tag{47}$$

We find an increment of mass flow rates

$$\Delta G_A = -G_0 \cdot \Delta Y. \tag{48}$$

Upon finding the increments, we find an increment of parameters:

$$t = t_1 - \Delta t, \tag{49}$$

$$Y = Y_1 - \Delta Y, \tag{50}$$

$$\vartheta = \vartheta_1 - \Delta\vartheta. \tag{51}$$

The mass share of ammonia in AWS is calculated considering ammonia evaporation (48) in SGM

$$y' = \frac{G_A - \Delta G_A}{G_{A(1)} + G_{W(1)} - \Delta G_A}. \tag{52}$$

The calculation is carried out by successive increments of the parameters until the specified value of AWS purification is reached.

It is obvious that the calculation is more accurate, the smaller the increments Δx.

To calculate the ARU solution vaporizer, it is necessary to have a database of initial data that could only be obtained during experimental studies of actual models.

Taking into consideration the results obtained in the experimental studies and using known ratios for the processes of heat-mass exchange, an estimate was made of the structural size of the solution vaporizer as part of ARU with a cooling capacity from 15 to 75 W.

In accordance with the methodology given in [41], we determined the geometric parameters of AWS jet: the equivalent diameter of the jet; the length of the arc of the heat-mass exchange surface; the cross-sectional area of the jet; the volumetric flow rate of a liquid; average speed; the length of the chord of the jet; Reynolds' number.

The diffusion Nusselt number for the flow of the liquid phase in a jet is determined by taking into consideration the range of AWS current modes in ARU film absorbers [42]:

$$Nu'_L 0.05 \cdot \mathrm{Re}_L \cdot \mathrm{Pr}_L^{0.5}. \tag{53}$$

To calculate the mass exchange process in SGM at evaporation, one can use the criterion equation in the form given in [43]:

$$Nu'_G = 0.6 \cdot \mathrm{Re}_G^{0.576} \cdot \left(\mathrm{Pr}'_G\right)^{0.5} \cdot \left(\frac{d}{l}\right)^{-0.2}. \tag{54}$$

The mass transfer factor in the process of ammonia evaporation from AWS [44] is:

$$K_A = \frac{1}{\frac{1}{\beta_y} + \frac{m}{\beta_x}}. \tag{55}$$

The results of the calculations based on the above algorithm are shown in Fig. 4.

The calculation was carried out in the range of the thermal capacity of standard ARU generators, 70...150 W [45], the mass flow rate of strong AWS is $(13...24)\cdot 10^{-5}$ kg/s, the flow of weak AWS – $(9...19)\cdot 10^{-5}$ kg/s.

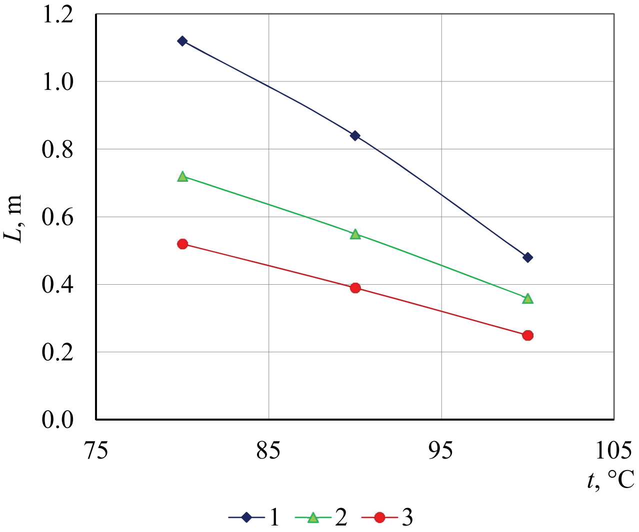

Fig. 4. The results of calculating the solution vaporizer as part of ARU at various heat loads on the generator-thermosyphon, temperature, and formulation of weak AWS at the inlet: 1 – 70 W; 2 – 100 W; 3 – 150 W; at 80 °C, the mass share of AWS is 0.58; at 90 °C, the mass share of AWS is 0.51; at 100 °C, the mass share of AWS is 0.44

7. Discussion of results of studying ARU operated from low-potential thermal energy sources

In this paper, we have studied the source of artificial cold as part of the system for obtaining water from atmospheric air of the absorption type. Testing was carried out on the possible use of upgraded ARU [20] with a low-potential heat source under actual climatic operational modes of the systems for obtaining water from atmospheric air [24]. For this study, an authentic algorithm was developed to analyze the thermodynamic processes of the ARU cycle, characteristic of the systems for obtaining water from atmospheric air. These are the processes of ammonia evaporation into the vapor gas environment at low (0.3...0.5 MPa) and high (up to 1.0 MPa) partial pressure; the absorption of ammonia vapor at elevated AWS temperatures; the evaporation of a steam mixture at temperatures of 70–100 °C.

In contrast to other researchers [8, 27–35], this paper has used the specific mass flow rates of the components of the working body: ammonia; water; hydrogen. That has simplified the analysis and made it more illustrative.

The second feature of the calculation algorithm was the boundary conditions on the formulation of the working body at the characteristic points of the ARU cycle.

It has been shown that in order to ensure the predetermined mode of operation of the solution vaporizer and to prevent partial absorption, it is necessary to maintain the temperature in it almost at the level of the boiling end in the generator (25). In practice, it is possible to minimize thermal losses in the environment by installing an appropriate insulation coating.

For more accurate calculations of the operational mode of the solution vaporizer, one should take into consideration the contribution of the cold flow SGM, which must be calculated using the appropriate equations of heat and mass exchange (26) to (32), (53) to (55).

However, we are not aware of either theoretical or experimental work on the process of heat and mass exchange in the evaporation of ammonia from an ammonia-water solution into a steam-gas mixture.

The analog here is likely the reverse process – the absorption of ammonia vapor from a steam gas mixture with an ammonia-water solution.

Taking this analogy into consideration, we simulated the processes of heat and mass exchange in the solution vaporizer, which showed that an increase in heat load in the heat supply zone, accompanied by an increase in the temperature of generation, increases the amount of a circulating working body and leads to the need to increase the surfaces of the heat and mass exchange (Fig. 4).

Our calculations have shown that an increase in the mass proportion of ammonia in weak AWS at the inlet of the solution vaporizer also requires an increase in its surface. Thus, with a mass proportion of ammonia of 0.58 in weak AWS, compared to 0.44, it requires on average an increase of 2.2 times in its surface of heat and mass exchange.

As demonstrated by the variant calculation (Fig. 4), the proposed modification of ARU with an adiabatic solution vaporizer could work as part of the systems for obtaining water from atmospheric air at hot spring temperatures of 100 °C, and constructively enough fits into the element base of standard models. On average, the solution vaporizer is about 10 % of the surface of the absorber.

Despite the positive experience of the use in the structures of absorbers and vaporizers of ammonia in ARU of the radial capillary notch, further studies of ARU must investigate the extent of its effect on the heat and mass exchange processes in the evaporation of the solution in SGM.

However, no possibility of using, for the ARU model described in [20], low-cost solar collectors with water as a heat carrier was found. Under the actual climatic conditions of operation of the systems for obtaining water from atmospheric air, it is necessary, at least, to ensure a boiling point of 90 °C.

In the actual execution of ARU, taking into consideration thermal losses and thermal resistance in the contact zone between the heat source and the wall of the ARU generator, one should expect even high temperatures.

At the same time, estimates have shown that under the conditions of moderate ambient temperatures (20...22 °C), as well as when cooling the capacitor with water, when the working pressure in the system could be reduced to 1.0...1.2 MPa, the ARU could be operated at 80 °C.

Thus, we can recommend two types of ARU [20] thermal load source as part of the systems for obtaining water from atmospheric air for designers:

– in a tropical hot climate, with vacuum solar collectors or solar hubs capable of providing temperatures above 200 °C [11].

– in a temperate climate zone, with solar collectors where water is a heat carrier [11].

The energy efficiency of the ARU cycle was not calculated in this work as it is assumed that water production systems would utilize alternative sources of thermal energy.

It is obvious that, compared to analogs, ARU with a solution vaporizer (Fig. 1) would have large mass-dimension characteristics. At the same time, there is reason to believe that it is possible to partially eliminate this deficiency by developing a scheme with the supply to the solution vaporizer of the flow of purified SGM from the absorber. In that case, SGM flow should be paralleled (position 7, Fig. 2).

8. Conclusions

1. We have analyzed the thermodynamic processes in ARU, capable of working at lower, compared to analogs, temperatures of the thermal energy source. The possibility of reducing the temperature level of the heat source by including a solution vaporizer in the ARU scheme has been studied. The analysis involved an authentic method based on the balance of the specific streams of ARU working body components and boundary conditions at characteristic points of the cycle. A limitation on the level of minimum boiling temperatures in the ARU generator (from 90 °C) was shown when operating the systems for obtaining water from atmospheric air in harsh climatic conditions (an ambient air temperature of 32 °C and above).

2. The structure of ARU with an adiabatic solution vaporizer, proposed on the basis of our analysis, could work as part of the systems for obtaining water from atmospheric air at hot spring temperatures of 100 °C and constructively enough fits into the element base of standard models. On average, the solution vaporizer is about 10 **%** of the surface of the absorber.

It is proposed to utilize two types of thermal energy sources for the operation of ARU as part of the systems for obtaining water from atmospheric air. In a tropical climate, it is recommended to use a thermal energy source based on vacuum solar collectors or solar energy concentrators, and, in a temperate climate zone, based on solar collectors with water as a heat carrier.

References

1. Mehanizm «OON – vodnye resursy». Mezhdunarodnoe desyatiletie deystviy «Voda dlya zhizni», 2005-2015 gody. Available at: http://www.un.org/ru/waterforlifedecade/unwater.shtml
2. Thimmaraju, M., Sreepada, D., Babu, G. S., Dasari, B. K., Velpula, S. K., Vallepu, N. (2018). Desalination of Water. Desalination and Water Treatment. doi: https://doi.org/10.5772/intechopen.78659
3. Al' Maytami Valid Abdulvahid Mohammed, Frumin, G. T. (2007). Directions of perfection of water supply in the countries of the arabian peninsula. Modern problems of science and education, 6, 13–17. Available at: https://www.science-education.ru/ru/article/view?id=769
4. Salehi, A. A., Ghannadi-Maragheh, M., Torab-Mostaedi, M., Torkaman, R., Asadollahzadeh, M. (2020). A review on the water-energy nexus for drinking water production from humid air. Renewable and Sustainable Energy Reviews, 120, 109627. doi: https://doi.org/10.1016/j.rser.2019.109627
5. Al' Maytami Valid Abdulvahid Mohammed, Frumin, G. T. (2008). Ecologically safe technologies of water supply in the countries of arabian peninsula. Modern problems of science and education, 3, 111–115. Available at: https://www.science-education.ru/ru/article/view?id=764
6. Tu, Y., Wang, R., Zhang, Y., Wang, J. (2018). Progress and Expectation of Atmospheric Water Harvesting. Joule, 2 (8), 1452–1475. doi: https://doi.org/10.1016/j.joule.2018.07.015
7. Srivastava, S., Yadav, A. (2018). Water generation from atmospheric air by using composite desiccant material through fixed focus concentrating solar thermal power. Solar Energy, 169, 302–315. doi: https://doi.org/10.1016/j.solener.2018.03.089
8. Zolfagharkhani, S., Zamen, M., Shahmardan, M. M. (2018). Thermodynamic analysis and evaluation of a gas compression refrigeration cycle for fresh water production from atmospheric air. Energy Conversion and Management, 170, 97–107. doi: https://doi.org/10.1016/j.enconman.2018.05.016
9. The European Solar Thermal Industry Federation (ESTIF). Available at: http://www.estif.org/
10. Thermal solar line. Rotartica, air conditioning appliances: Solar Line, single effect 4,5kW. Available at: http://andyschroder.com/static/pdf/Rotartica/Rotartica_Product_Description.pdf
11. Perel'shteyn, B. H. (2008). Novye energeticheskie sistemy. Kazan': Izd-vo Kazan. gos. tehn. un-ta, 208.
12. Vasyliv, O. B., Kovalenko, O. O. (2009). Struktura ta shliakhy ratsionalnoho vykorystannia vody na kharchovykh pidpryiemstvakh. Naukovi pratsi ONAKhT, 35, 54–58.
13. Elsheniti, M. B., Elsamni, O. A., Al-dadah Raya K., Mahmoud, S., Elsayed, E., Saleh, K. (2018). Adsorption Refrigeration Technologies. Sustainable Air Conditioning Systems. doi: https://doi.org/10.5772/intechopen.73167
14. Vasyliv, O. B., Titlov, O. S., Osadchuk, Ye. O. (2015). Pat. No. 100195 UA. Sposib oderzhannia vody z atmosfernoho povitria. No. u201501512; declareted: 20.02.2015; published: 10.07.2015, Bul. No. 13. Available at: https://uapatents.com/7-100195-sposib-oderzhannya-vodi-z-atmosfernogo-povitrya.html
15. Busso, A., Franco, J., Sogari, N., Cáceres, M. (2011). Attempt of integration of a small commercial ammonia-water absorption refrigerator with a solar concentrator: Experience and results. International Journal of Refrigeration, 34 (8), 1760–1775. doi: https://doi.org/10.1016/j.ijrefrig.2011.07.004
16. Gutiérrez, F. (1988). Behavior of a household absorption-diffusion refrigerator adapted to autonomous solar operation. Solar Energy, 40 (1), 17–23. doi: https://doi.org/10.1016/0038-092x(88)90067-9
17. Osadchuk, E. A., Titlov, A. S., Mazurenko, S. Yu. (2014). Determination of power efficient operating conditions of absorption water-ammonia refrigerating machine in the systems for obtaining water from atmospheric air. Refrigerating and accompanying technologies, 50 (4), 54–57. doi: https://doi.org/10.15673/0453-8307.4/2014.28054
18. Osadchuk, E., Titlov, A., Kuzakon, V., Shlapak, G. (2015). Development of schemes of pump and gasoline-pump absorption water-ammonia refrigeration machines to work in a system of water production from the air. Technology audit and production reserves, 3 (3 (23)), 30–37. doi: https://doi.org/10.15587/2312-8372.2015.44139

19. Osadchuk, E. A., Titlov, A. S., Vasyliv, O. B., Mazurenko, S. Yu. (2014). Poisk energeticheski effektivnostivnyh rezhimov raboty absorbtsionnoy vodoammiachnoy holodil'noy mashiny v sistemah polucheniya vody iz atmosfernogo vozduha. Naukovi pratsi ONAKhT, 1 (45), 65–69.
20. Gerhard, K. (1999). Pat. No. 57849 UA. Absorption cooling machine. No. 2001031479; declareted: 03.09.1999; published: 15.07.2003, Bul. No. 7. Available at: https://uapatents.com/7-57849-absorbcijjna-kholodilna-mashina.html
21. Natural Refrigerants. Available at: https://www.linde-gas.com/en/products_and_supply/refrigerants/natural_refrigerants/index.html
22. Hobin, V. A., Titlova, O. A. (2014). Energoeffektivnoe upravlenie absorbtsionnymi holodil'nikami. Kherson: Grin' D.S., 216.
23. Tiukhai, D. S. (1999). Poshuk enerhozberihaiuchykh rezhymiv roboty absorbtsiyne-dyfuziynoi tekhniky na bazi unifikovanoi ADKhM. Naukovi pratsi ONAKhT, 20, 229–234.
24. Osadchuk, Ye., Titlov, O. (2020). Search for energy efficient modes of systems operation for obtaining water from atmospheric air on the basis of absorption water-ammonia thermal transformers of heat and solar collectors. Refrigeration Engineering and Technology, 56 (3-4), 78–91. doi: https://doi.org/10.15673/ret.v56i3-4.1951
25. Titlov, A. S. (2008). Povyshenie energeticheskoy effektivnosti absorbtsionnyh holodil'nyh priborov. Naukovi pratsi ONAHT, 1 (34), 295–303.
26. Ishchenko, I. M., Titlov, O. S. (2018). Improvement of regime parameters of water-absorbing ammonia refrigeration units operating in a wide range of ambient temperatures. Refrigeration Engineering and Technology, 54 (3), 10–20. doi: https://doi.org/10.15673/ret.v54i3.1096
27. Galimova, L. I. (1997). Absorbtsionnye holodil'nye mashiny i teplovye nasosy. Astrahan', 226.
28. Ischenko, I. N. (2010). Modelirovanie tsiklov nasosnyh i beznasosnyh absorbtsionnyh holodil'nyh agregatov. Naukovi pratsi ONAKhT, 2 (38), 393–405.
29. Morozyuk, T. V. (2006). Teoriya holodil'nyh mashin i teplovyh nasosov. Odessa: Studiya «Negotsiant», 712.
30. Mazouz, S., Mansouri, R., Bellagi, A. (2014). Experimental and thermodynamic investigation of an ammonia/water diffusion absorption machine. International Journal of Refrigeration, 45, 83–91. doi: https://doi.org/10.1016/j.ijrefrig.2014.06.002
31. Jemaa, R. B., Mansouri, R., Boukholda, I., Bellagi, A. (2016). Experimental investigation and exergy analysis of a triple fluid vapor absorption refrigerator. Energy Conversion and Management, 124, 84–91. doi: https://doi.org/10.1016/j.enconman.2016.07.008
32. Mansouri, R., Bourouis, M., Bellagi, A. (2017). Experimental investigations and modelling of a small capacity diffusion-absorption refrigerator in dynamic mode. Applied Thermal Engineering, 113, 653–662. doi: https://doi.org/10.1016/j.applthermaleng.2016.11.078
33. Yıldız, A., Ersöz, M. A. (2013). Energy and exergy analyses of the diffusion absorption refrigeration system. Energy, 60, 407–415. doi: https://doi.org/10.1016/j.energy.2013.07.062
34. Ben Jemaa, R., Mansouri, R., Boukholda, I., Bellagi, A. (2017). Experimental characterization and performance study of an ammonia–water–hydrogen refrigerator. International Journal of Hydrogen Energy, 42 (13), 8594–8601. doi: https://doi.org/10.1016/j.ijhydene.2016.06.150
35. Taieb, A., Mejbri, K., Bellagi, A. (2016). Detailed thermodynamic analysis of a diffusion-absorption refrigeration cycle. Energy, 115, 418–434. doi: https://doi.org/10.1016/j.energy.2016.09.002
36. Ersöz, M. A. (2015). Investigation the effects of different heat inputs supplied to the generator on the energy performance in diffusion absorption refrigeration systems. International Journal of Refrigeration, 54, 10–21. doi: https://doi.org/10.1016/j.ijrefrig.2015.02.013
37. Jelinek, M., Levy, A., Borde, I. (2016). The influence of the evaporator inlet conditions on the performance of a diffusion absorption refrigeration cycle. Applied Thermal Engineering, 99, 979–987. doi: https://doi.org/10.1016/j.applthermaleng.2016.01.152
38. Srikhirin, P., Aphornratana, S. (2002). Investigation of a diffusion absorption refrigerator. Applied Thermal Engineering, 22 (11), 1181–1193. doi: https://doi.org/10.1016/s1359-4311(02)00049-2
39. Bogdanov, S. N., Burtsev, S. I., Ivanov, O. P., Kupriyanova, A. V. (1999). Holodil'naya tehnika. Konditsionirovanie vozduha. Svoystva veschestv. Sankt-Peterburg: SPbGAHPT (Sankt-Peterburgskaya gosudarstvennaya akademiya holoda i pischevyh tehnologiy), 320.
40. Osadchuk, E. A., Titlov, A. S. (2011). Analiticheskie zavisimosti dlya rascheta termodinamicheskih parametrov i teplofizicheskih svoystv vodoammiachnogo rastvora. Naukovi pratsi ONAKhT, 1 (39), 178–182.
41. Titlov, A. S., Vasylsv, O. B., Adambaev, D. B. (2018). Modeling of the manual non-stopped current modes of the liquid phase of the working body in the elements of absorption refrigerating devices. Refrigeration Engineering and Technology, 54 (3), 21–32. doi: https://doi.org/10.15673/ret.v54i3.1108
42. Osipov, Yu. V., Tret'yakov, N. P., Nekrasov, N. N. (1971). Teplo- i massoobmen pri absorbtsii ammiaka vodoammiachnym rastvorom iz vodoammiachnoy smesi. Holodil'naya tehnika, 9, 47–50.
43. Du, S., Wang, R. Z., Lin, P., Xu, Z. Z., Pan, Q. W., Xu, S. C. (2012). Experimental studies on an air-cooled two-stage NH_3-H_2O solar absorption air-conditioning prototype. Energy, 45 (1), 581–587. doi: https://doi.org/10.1016/j.energy.2012.07.041
44. Galimova, L. V., Vedeneeva, A. I. (2014). Scientific and practical foundations of removal of application to serving absorption water-ammonia chiller. Nauchniy zhurnal NIU ITMO. Seriya «Holodil'naya tehnika i konditsionirovanie», 1. Available at: https://cyberleninka.ru/article/n/nauchno-prakticheskie-osnovy-protsessa-absorbtsii-s-primeneniem-k-deystvuyuschey-absorbtsionnoy-vodoammiachnoy-holodilnoy-mashiny
45. Kaynakli, O., Yamankaradeniz, R. (2007). Thermodynamic analysis of absorption refrigeration system based on entropy generation. Current Science, 92 (4), 472–479.